IEEE Access
Multidisciplinary | Rapid Review | Open Access Journal

Received February 4, 2020, accepted February 24, 2020, date of publication March 3, 2020, date of current version March 16, 2020.

Digital Object Identifier 10.1109/ACCESS.2020.2977936

QoE Probability Coverage Model of Indoor Visible Light Communication Network

JUAN LI[1], XU BAO[1], WANCE ZHANG[1], AND NAN BAO[2]
[1]School of Computer Science and Communication Engineering, Jiangsu University, Zhenjiang 212013, China
[2]College of Internet of Things, Nanjing University of Posts and Telecommunications, Nanjing 210023, China

Corresponding author: Xu Bao (xbao@ujs.edu.cn)

This work was supported in part by the Key Research and Development Plan of Jiangsu Province under Grant BE2018108, in part by the National Natural Science Foundation of China under Grant 61772243, Grant 61701198, and Grant 61701255, in part by the Nature Science Foundation of Jiangsu Province under Grant BK20170557, and in part by the Young Talent Project of Jiangsu University.

ABSTRACT As a candidate wireless communication technology in future, visible light communication (VLC) not only provides the green illumination, but also transmits data at high speed without occupying the existing radio frequency (RF) spectrum resources, hence it can offload the data traffic from the crowded RF network. However, achieving satisfying traffic service with probability almost approaching one inside an indoor scenario is not an effortless task in VLC networks. Several factors such as transmitted power, number of user equipments (UEs), and multiple access schemes affect the coverage probability. In this paper, we utilize the user quality of experience (QoE) as the system performance metric, and the QoE probability coverage model is proposed which the LED coverage area projecting on the ground, we attempt to achieve a satisfying QoE with a certain probability on UEs. We investigate how the factors including non-orthogonal multiple access (NOMA) scheme, user pairing scheme, UE density, power allocation methods etc. affect the reliable QoE probability coverage area which contributes to a VLC network deployment, multiple access protocols and handover schemes.

INDEX TERMS Visible light communication (VLC), non-orthogonal multiple access (NOMA), coverage probability, quality of experience (QoE).

I. INTRODUCTION

Visible light communication (VLC) [1]–[3] is an evolving communication technology that uses LEDs as transmitters to emit both the light and information signals by leveraging the broad license-free optical spectrum at wavelengths of 380-750nm [4]. Compared to radio frequency (RF) technology, VLC offers many advantageous features such as higher data rates [5], lower power consumption, unlicensed spectrum, and high security. Moreover, VLC can be safely used in sensitive environment such as aircrafts and hospitals [6].

Nonetheless, because of the line-of-sight (LOS) propagation of optical signals, just one LED has a limited coverage area. Hence, in order to ensure a full indoor area coverage and satisfactory illuminations, it is necessary for multiple LEDs to work at the same time. However, adjacent LEDs may overlap with each other, which inevitably cause inter-cell interference (ICI). Therefore, the analysis of indoor VLC coverage performance plays an crucial part in studying the optimal LEDs layout, VLC system resource allocation algorithm and network handover.

Coverage issues are extensively investigated in wireless sensor networks (WSNs) [7]. Yang *et al.* in [8], investigated ε-full coverage problem under the probabilistic sensing model in WSNs. They studied the mathematics relation between the coverage of two adjacent sensor nodes and transformed the ε-full coverage problem into the point coverage problem. In [9], Hari *et al.* studied the coverage problem in WSNs considering the border effects and derived the required minimum sensor density to ensure the quality of coverage. The k-coverage problem was proposed in [10], which required a selection of a minimum subset of nodes among the deployed ones such that each point in the target region was covered by at least k nodes. Instead of the simplistic disk coverage model, the confident information coverage (CIC) model, which was based on the theory of field reconstruction, had been proposed for different types of sensor coverage

The associate editor coordinating the review of this manuscript and approving it for publication was Maurice J. Khabbaz.

studies [11], [12]. In [11], the authors discussed the sensor placement problem to achieve both coverage and connectivity on the basis of the CIC model. The critical sensor density to achieve complete coverage in randomly deployed sensor networks was studied in [12]. And this paper proposed a numerical computation method called discrete approximation algorithm (DAA) to compute the probability that an arbitrary point was not covered by randomly deployed sensors within its corresponding range. Similar to VLC, ultra dense RF network is also a candidate technology in future communication system. In [13], the author focused on using Poisson clustered process (PCP) to model ultra-dense 5G heterogeneous cellular networks which include macrocells, picocells and femtocells. In [14], it analyzed the ergodic throughput of the network where small base stations (SBSs) had limited backhaul capacity to accomplish flexible coverage with limited backhaul. In [15], the authors considered the model which incorporated multi-slope path loss and general fading distributions. They derived the tail behavior and scaling laws for the coverage probability and the capacity considering strongest base station association in a Poisson field network. Expectedly, in the next decade, ultra dense networks, with small cells, will cover most of indoor and outdoor spaces, providing data rate of 100 Mbps to cell edge users [16]. However, this will result in an increase in frequency reuse and will generate intolerable interference, limiting the spectral efficiency of the system. In this respect, VLC is envisioned to play a vital role in addressing these challenges, owing to its unique characteristics, such as unlicensed optical spectrum.

Due to the fundamental differences of the channel model between RF communication and VLC [3], the coverage research results of RF networks cannot be directly applied to VLC [17]. Hence, although there have been a lot of research results on WSN coverage and ultra dense RF network, VLC coverage is still an intriguing issue which has not been adequately studied. It is a challenge to achieve full coverage of an indoor environment due to its LOS transmission. Vavoulas *et al.* in [18], investigated the communication coverage of an indoor VLC network by considering the key factors such as error probability, power consumption, dimming, and node failure. An optimized circular deployment scheme was proposed in [19], which not only considered the position of LED transmitters on the ceiling, but also took into account the first reflections of each wall, so as to obtain more accurate results. In [20], a comprehensive investigation of both the illumination and communication coverage of an indoor MIMO-VLC system was presented. The MIMO-VLC system was assumed to be ICI-free with an ideal channel matrix. In [21], the coverage probability of a typical user was defined as the probability that its instantaneous signal to interference plus noise ratio (SINR) exceeded the target SINR threshold. For a VLC-only network, the coverage probability of a typical user depended on the probability that the optical base-stations (OBS) should be at least within the FOV of a typical user. The femtocell-like deployment of VLC in indoor environments leaded to the concept of optical attocells [22], a three-dimensional attocell model was considered in [23], and an analysis framework was introduced for coverage probability analysis in multi-user VLC networks. Shashikant proposed a method that simultaneously reduced the interference caused by multiple sources in indoor VLC system and improved the coverage area [24]. However, most research of VLC coverage issues only analyzed the impact of some quality of service (QoS) parameters on coverage performance, but did not discuss the effects of user equipments (UEs) accessing strategy, and resource allocation methods.

Non-orthogonal multiple access (NOMA) is a new technology nominated for the fifth generation (5G) wireless networks aimed at increasing the throughput, decreasing the latency, and improving the fairness and connectivity [25], [26]. Different types of NOMAs, such as the power domain NOMA (PD-NOMA), pattern division multiple access (PDMA), sparse code multiple access (SCMA), are presented as good candidates for the 5G multiple access technique. However, only PD-NOMA is implemented in VLC network based on different power levels set for different UEs. Because the PD-NOMA scheme is based on successive interference cancellation (SIC), NOMA-VLC networks require all UEs' channel state information (CSI) to be available, which is identical to the case in VLC. Kizilirmak *et al.* [27] and Lin *et al.* [28] demonstrated the superiority of NOMA over OFDMA, in VLC systems, with respect to sum rate and BER performance, respectively.

In this paper, we utilize quality of experience (QoE) as the evaluation metric to propose a QoE probability coverage model in NOMA-based VLC network. It is defined as the LED coverage area projecting on the ground that the UEs can achieve a satisfying QoE with a certain probability. Simultaneously, we investigate how the factors including UE density, power allocation (PA) methods, transmission power, number of UEs, etc., affect the QoE probability coverage performance. Simulations are carried out to verify the derived analytical solutions. The main contributions of this paper are summarized as follows.

1) We propose a QoE probability coverage model by using QoE as the evaluation metric in multi-user VLC networks. Specifically, coverage probability of the VLC access point (AP) is defined as the probability that the QoE values of all UEs in the coverage area exceeds the threshold Q_t.
2) By assuming that multiple UEs are randomly distributed in the coverage area, the VLC coverage performance is evaluated by adopting NOMA with/without user pairing in the proposed QoE probability coverage model. The simulation results manifest the impact of factors such as UE density, number of UEs, and transmission power, etc., on the coverage performance.
3) Based on the derivation of single cell coverage probability, the QoE coverage radius of fixed coverage probability is obtained. Furthermore, we achieve the

coverage ratio under the multi-cell scenarios to analyze the overall indoor coverage performance.

The rest of this paper is organized as follows. Section II introduces VLC channel model, QoE definition and the QoE probability coverage model. The QoE coverage performance in VLC network is evaluated in Section III. In Section IV, we assess the QoE coverage ratio for multiple cells. The simulation results are presented and discussed in Section V. Finally, the Section VI draws conclusion.

II. SYSTEM MODEL

A. CHANNEL MODEL

Fig. 1 and Fig. 2 illustrate the conceptual VLC downlink system. We consider an indoor scenario deployed with the LED bulbs that are mounted on the ceiling and N UEs that are scattered uniformly. The VLC receivers that are held by UEs are assumed to be parallel with the ceiling. The vertical distance between the receiver plane and the LED transmitter is L, which is a constant in this paper. The transmitter model employs a Lambertian optical source, of which the brightness to an observer is the same regardless of the observer's angle of view [29]. Besides, only the LOS transmitter downlink between LEDs and the receivers are considered because the reflected or diffuse optical path loss is about 110-120 dB larger than the path loss of the LOS transmission [30]. A typical indoor environment usually comprises multiple adjacent LEDs which form bordering or overlapping VLC cells, as shown in Fig. 2.

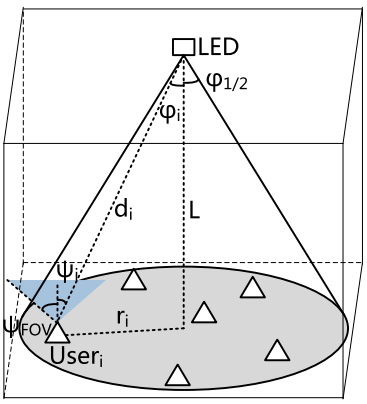

FIGURE 1. Single cell system model.

The i-th UE direct current (DC) channel gain is given by [31]

$$h_i = \begin{cases} \frac{E}{d_i^2}\cos^m(\varphi_i)\cos(\psi_i), & 0 < \psi_i \le \psi_{FOV} \\ 0, & \psi_i > \psi_{FOV}, \end{cases} \tag{1}$$

where m is the order of Lambertian emission, depending on the semi-angle $\varphi_{1/2}$ at half illuminance of the LED, which is given by $m = -1/log_2(\cos(\varphi_{1/2}))$. ψ_{FOV} denotes the field-of-view (FOV) of a receiver, φ_i and ψ_i are the angles of irradiance and incidence, respectively. d_i denotes the Euclidean

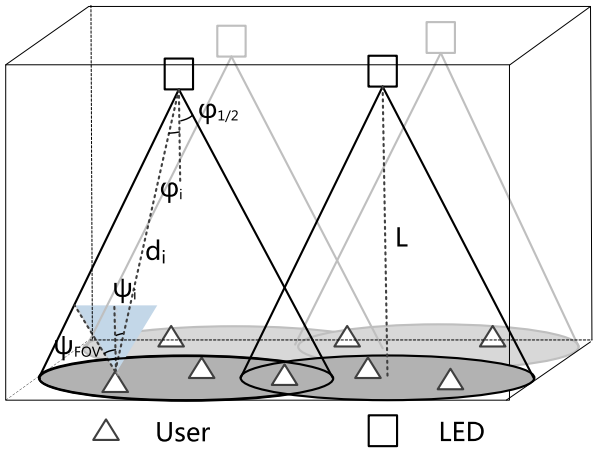

FIGURE 2. Multiple cells system model.

distance between the LED and the i-th UE, $d_i = \sqrt{r_i^2 + L^2}$, where r_i is the projection distance as shown in Fig. 1. The E represents

$$E = \frac{A(m+1)}{2\pi} T_s(\psi_i)\, g(\psi_i), \tag{2}$$

$T_s(\psi_i)$ is the gain of the optical filter, and $g(\psi_i)$ represents the gain of the optical concentrator given by [31]

$$g(\psi_i) = \begin{cases} \frac{n^2}{\sin^2(\psi_{FOV})}, & 0 < \psi_i \le \psi_{FOV} \\ 0, & \psi_{FOV} \le 0, \end{cases} \tag{3}$$

where n is the refractive index.

We investigate the NOMA transmission for the VLC downlink. Multiple UEs with sufficient different channel qualities are served simultaneously on the same lightwave band, which results in a non-orthogonal transmission strategy. In NOMA, UEs are multiplexed in the power domain by using superposition coding at the transmitter side and successive interference cancellation (SIC) at the receivers [25][26].

Without loss of generality, the channels are sorted as $|h_1^2| \le |h_2^2| \le \ldots \le |h_i^2| \le \ldots \le |h_N^2|$. According to the power domain NOMA principle, the superposed signal to be transmitted at the LED is given by [32]

$$x_i = \sum_{i=1}^{N} a_i \sqrt{P} s_i + I_{DC}, \tag{4}$$

where the total electrical power of all the message signals is P, $P = \sum_{i=1}^{N} P_i$, s_i is the modulated message signal intended for the i-th UE. a_i is the power allocation factor, it must be satisfied $\sum_{i=1}^{N} a_i^2 = 1$ because of the total power constraint. I_{DC} is the DC bias added to the LED to ensure the positive instantaneous intensity. After removing the DC term, the received signal at the i-th UE is formed by the contribution of all signals transmitted from the LED, written as [32]

$$y_i = \sqrt{P} h_i \left\{ \sum_{l=1}^{i-1} a_l s_l + a_i s_i + \sum_{j=i+1}^{N} a_j s_j \right\} + z_i, \tag{5}$$

where h_i is the direct current (DC) channel gain for the i-th UE, defined as eq. (1). z_i denotes the real-valued Gaussian noise with zero mean and variance $\sigma_i^2 = N_0 B$, N_0 is noise power spectral density (PSD), B is the signal bandwidth.

At the receiver side, it will perform SIC [26]. In the process of SIC, the i-th UE will detect the l-th UE's message, $l < i$, and then remove the message from its observation, in a successive manner. The signal of the j-th UE, $j > i$, will be treated as noise at the i-th UE. According to (5), the achievable rate of the i-th UE is given by

$$R_i = \begin{cases} \log_2 \left[1 + \dfrac{(h_i a_i)^2}{\sum\limits_{j=i+1}^{N} (h_i a_j)^2 + 1/\rho} \right], & i = 1, \cdots, N-1 \\ \log_2 \left[1 + \rho (h_i a_i)^2 \right], & i = N, \end{cases} \tag{6}$$

where $\rho = P/(N_0 B)$ represents the transmitting signal-to-noise radio (SNR).

B. QUALITY OF EXPERIENCE

Quality of experience (QoE) ties together user perception, experience, and expectations to application and network performance, typically expressed by quality of service (QoS) parameters. QoE metrics attempt to characterize the match between user needs and content delivered. A high network QoS cannot always assure a high QoE. Compared to QoS, QoE can better reflects user satisfaction. The quantification of QoE, which is currently widely used is Mean Opinion Score (MOS) [33]. QoE can be determined through subjective ratings by real users or predicted from objective measurements of properties of the delivered goods such as audio, video, or files. As shown in Table 1, it divides the subjective feelings of QoE into five levels in terms of user satisfaction, represented by MOS scores.

TABLE 1. Mean opinion score.

Score	User Satisfaction
5	Excellent
4	Good
3	Fair
2	Poor
1	Bad

For audio traffic, the QoE function Q_{audio} is defined by a nonlinear mapping of the R factor:

$$Q_{audio}\left(R_f\right) = 1 + 0.035 R_f + 7 \times 10^{-6} \times R_f \left(R_f - 60\right)\left(100 - R_f\right), \tag{7}$$

where R_f is the R factor defined by ITU to reflect the audio quality impairment from different aspects [34], [35]. In video traffic, the MOS primarily depends only on the loss of a slice of frame from the video stream [36]. The MOS can be simplified as a function of the peak signal-to-noise ratio (PSNR) with some transformation [37]. The QoE function Q_{video} is given as

$$Q_{video}\left(P_{snr}\right) = 4.5 - \frac{3.5}{1 + \exp\left(b_1 \left(P_{snr} - b_2\right)\right)}, \tag{8}$$

where b_1 and b_2 are the parameters determining the shape of the function and P_{snr} is the experienced PSNR. Traffic such as file transfer and web browsing in non-real-time are called elastic traffic. The corresponding QoE is defined as an increasing function of throughput R

$$Q_{elastic}\left(R\right) = b_3 \log_{10}\left(b_4 R\right), \tag{9}$$

where b_3 and b_4 are determined by the required maximal and minimal throughput [38]. VLC is suitable for downlink high-speed data transmission, therefore, we only consider elastic traffic in this paper, the corresponding QoE function is eq. (9). We can bring the maximum and minimum throughput (70 and 20 Mbps) into eq. (9), which respectively correspond to the MOS value of the 5 and 1 of QoE. Through calculation, the resulting parameters are given as $b_3 = 0.6476$ and $b_4 = 0.7503$.

C. QOE PROBABILITY COVERAGE MODEL

We utilize the UE QoE as the system performance metric. The QoE probability coverage model is proposed as the LED coverage area projecting on the ground that the UEs can achieve a satisfying QoE with a certain probability. The coverage probability of one UE is defined as the probability that its QoE exceeds the threshold Q_t. Based on (6) and (9), the coverage probability of the i-th UE can be expressed as

$$P_i^{cov} = P_r\left[QoE_i \geq Q_t\right], \tag{10}$$

where $P_r[\cdot]$ denotes the probability of an event, QoE_i represents the i-th UE QoE value at the current location, and Q_t is the minimum QoE value that the UE needs to satisfy.

We define $r_{max}^{P_t}$ as the maximum QoE coverage radius, given the coverage probability value P_t. In this coverage area, the QoE coverage probability of any UE exceeds the coverage probability threshold P_t,

$$r_{max}^{P_t} = \underset{\forall i \in U}{\arg} \left\{ P_i^{cov} > P_t \right\}, \tag{11}$$

where U denotes the UE set.

III. QOE PROBABILITY COVERAGE MODEL FOR SINGLE CELL

Based on the QoE probability coverage model that proposed in section II. C, we further derive the QoE coverage probability of one cell, given the number of UEs and the accessing mechanism of NOMA.

A. NOMA SCHEME WITHOUT USER PAIRING

By using NOMA for N UEs, according to (10) the coverage probability of the i-th UE is written as

$$P_i^{cov} = P_r\left[b_3 \log_{10}\left(b_4 R_i\right) \geq Q_t\right]. \tag{12}$$

As can be seen from Fig. 1, the relationship between φ_i, ψ_i, L, r_i, the $\cos(\varphi_i)$ and $\cos(\psi_i)$ can be written as

$$\cos(\varphi_i) = \cos(\psi_i) = \frac{L}{\sqrt{r_i^2 + L^2}}, \tag{13}$$

therefore, based on (1), the optical channel gain h_i can be written as

$$h_i = \frac{\Gamma}{\left(r_i^2 + L^2\right)^{(m+3)/2}}, \tag{14}$$

where $\Gamma = EL^{m+1}$, E is defined in eq. (2), L is the vertical distance between the receiver plane and the LED transmitter, which is a constant in this paper.

According to the (6), (12) and (14), the QoE coverage probability can be expressed as

$$P_i^{cov} = P_r\left[r_i \le \left\{\left[\frac{\xi}{\left(\Gamma^2\rho\right)V}\right]^{\frac{-1}{m+3}} - L^2\right\}^{\frac{1}{2}}\right], \tag{15}$$

where $\xi = 2^{(1/b_4)\cdot 10^{Q_t/b_3}} - 1$, $V = a_i^2 - \xi\sum_{j=i+1}^{N} a_j^2$, a_i and a_j are the i-th UE's and the j-th UE's power allocation factors, respectively.

As shown in Fig. 1, the i-th UE's horizontal separation distance from the LED is represented r_i. We assume the UEs are uniformly distributed in the disc coverage area with radius r_{max}. The probability density function (PDF) of r_i following uniform distribution is expressed as

$$f(r_i) = \frac{2r_i}{r_{max}^2}. \tag{16}$$

We define the network coverage probability as a probability threshold P_{cov} that any UE with the coverage area can satisfy the condition $P_i^{cov} \ge P_{cov}$. According to (16), (15) can be written as

$$P_i^{cov} = \int_0^{\zeta} \frac{2r_i}{r_{max}^2} dr_i = \frac{\zeta^2}{r_{max}^2} \ge P_{cov}, \tag{17}$$

where ζ is denoted as

$$\zeta = \left\{\left[\frac{\xi}{\left(\Gamma^2\rho\right)V}\right]^{\frac{-1}{m+3}} - L^2\right\}^{\frac{1}{2}}. \tag{18}$$

If we obtain the equal sign in (17), the network coverage probability can be obtained as

$$P_{cov} = \frac{1}{r_{\max}^2}\left\{\left[\frac{\xi}{\left(\Gamma^2\rho\right)V}\right]^{\frac{-1}{m+3}} - L^2\right\}. \tag{19}$$

Given a certain network coverage probability, the QoE coverage radius can be written as

$$r_{\max}^{P_t} = \left(\frac{1}{P_{cov}}\left\{\left[\frac{\xi}{\left(\Gamma^2\rho\right)V}\right]^{\frac{-1}{m+3}} - L^2\right\}\right)^{\frac{1}{2}}. \tag{20}$$

B. USER PAIRING SCHEME

Since multiple UEs are served in NOMA system, co-channel interference are severe. Because of interference constraints, it is impractical to accommodate a large group of UEs. In [39], the author pointed out that for larger numbers of UEs, particularly, in a small cell size, the channel conditions might not differ significantly among UEs. Hence, it is difficult to utilize VLC to handle too many UEs at the same time in the receiver side. In this case, a hybrid scheme combined OMA and NOMA is suitable to fulfill a better trade-off between capacity and reliability. Specifically, the UEs in the system can be divided into different groups. Different groups are allocated with orthogonal bandwidth resources, where NOMA is implemented within each group [40].

Without loss of generality, the c-th and the d-th UE, $c < d$, are selected in pair to perform NOMA where c-th UE is farther away from the center of the coverage area. So, the channel gain of d-th UE is larger than the one of the c-th UE. a_c and a_d represent the power allocation factors for the two UEs respectively. According to the principle of NOMA, $a_c > a_d$ since $|h_c|^2 \le |h_d|^2$, and the restraint is $a_c^2 + a_d^2 = 1$. Then the rates achievable of the two UEs are given by [27]

$$\begin{cases} R_c = \log_2\left[1 + \dfrac{(h_c a_c)^2}{(h_c a_d)^2 + 1/\rho}\right] \\ R_d = \log_2\left[1 + \rho(h_d a_d)^2\right]. \end{cases} \tag{21}$$

For the UEs with user pairing, the QoE jointly coverage probability of two UEs can be written as

$$P_{cd} = P_r\left[QoE_c \ge Q_t, QoE_d \ge Q_t\right]. \tag{22}$$

To simplify the calculation of eq. (22), we consider further analysis of the relationship between two UEs. Lemma 1 below resolves this issue by comparing the QoE of two paired UEs.

Lemma 1: When we adopt the power allocation method with the factor of a_i, where $a_i = \sqrt{2(N-i+1)/(N(N+1))}$ [32], if the c-th UE which is far from the center of the coverage area satisfies the condition of QoE_c exceeding the threshold Q_t, the d-th UE which is close to the center must also satisfies the condition of QoE_d exceeding the threshold Q_t.

Proof: The QoE of c-th UE and d-th UE satisfy $\min\{QoE_c, QoE_d\} \ge Q_t$, and we assume that the QoE_c is less than the QoE_d. If the hypothesis condition is true, Lemma 1 is true. The QoE inequality of two UEs is given by

$$QoE_c < QoE_d. \tag{23}$$

According to the (9), (23) can be expressed as

$$b_3\log_{10}(b_4R_c) < b_3\log_{10}(b_4R_d), \tag{24}$$

where the expression of R_c and R_d are obtained as in (21), so (24) can be written as

$$\frac{(h_c a_c)^2}{(h_c a_d)^2 + \frac{1}{\rho}} < \rho(h_d a_d)^2. \tag{25}$$

We apply reasonable transformation to both sides of (25), which can be expressed as

$$\left(\frac{h_c}{h_d}\right)^2\left(\frac{a_c}{a_d}\right)^2 < \rho(h_c a_d)^2 + 1. \tag{26}$$

a_c and a_d are the power allocation factors of NOMA, $a_c^2 + a_d^2 = 1$, so we have $0 < a_c^2 < 1$ and $0 < a_d^2 < 1$. According to [32], the power allocation factors $a_i = \sqrt{2(N-i+1)/(N(N+1))}$, therefore

$$\left(\frac{a_c}{a_d}\right)^2 = \frac{2\,(N-c+1)}{N\,(N+1)} \times \frac{N\,(N+1)}{2\,(N-d+1)} = \frac{N-c+1}{N-d+1}, \tag{27}$$

where $c < d \leq N$, so $1 < \left(\frac{a_c}{a_d}\right)^2 < 2$. $\rho = \frac{P}{N_0 B}$ represents the transmitting SNR. In general, the value of power P ranges from $0.1W$ to $10W$, bandwidth B is around $10MHz$ to $20MHz$, $N_0 = 10^{-21}A^2/Hz$. As a result, the magnitude of ρ is about 10^{14}. Based on the eq. (1), (2), (3),

$$h_i = \frac{A\,(m+1)}{2\pi d_i^2}\cos^m(\varphi_i)\,T_s(\psi_i)\,g(\psi_i)\cos(\psi_i). \tag{28}$$

In general, $A = 1cm^2$, $m = -1/\log_2\left(\cos\left(\varphi_{1/2}\right)\right)$, $\varphi_{1/2}$ is around $60°$ to $75°$, $T_s(\psi_i) = 1$, $g(\psi_i) = 3$, $d_i = \sqrt{r_i^2 + L^2}$, $\cos(\varphi_i) = \cos(\psi_i) = \frac{L}{\sqrt{r_i^2+L^2}}$, L ranges from $2m$ to $4m$, r_i ranges from 0 to $4m$. As a result, the magnitude of h_i is about 10^{-6}, $\left(\frac{h_c}{h_d}\right)^2$ ranges from 0 to 1, the magnitude of ρh_c^2 ranges from 10^2 to 10^4. So it is clear that inequality relationship of (26) is always true, namely, $QoE_c > QoE_d$ is always false. Hence Lemma 1.

According to Lemma 1, the calculation of the (22) can be simplified

$$P_{cd} = P_r\left[QoE_c \geq Q_t\right]. \tag{29}$$

The QoE coverage probability of user pairing can be obtained

$$P_{cd} = P_r\left[r_c \leq \left\{\left[\frac{\xi}{\left(\Gamma^2\rho\right)\left(a_c^2 - a_d^2\xi\right)}\right]^{\frac{-1}{m+3}} - L^2\right\}^{\frac{1}{2}}\right]. \tag{30}$$

Based on the (17), the QoE network coverage probability with user pairing is written as

$$P_{cov} = \frac{1}{r_{\max}^2}\left\{\left[\frac{\xi}{\left(\Gamma^2\rho\right)\left(a_c^2 - a_d^2\xi\right)}\right]^{\frac{-1}{m+3}} - L^2\right\}. \tag{31}$$

IV. QOE PROBABILITY COVERAGE MODEL FOR MULTIPLE CELLS

In this section, we further discuss the joint coverage performance of multiple cells. In order to simplify the analysis process, we assume that different lightwave bands are utilized in adjacent cells to avoid inter-cell interference. Therefore, the inter-cell interference between cells is not considered in this paper. Based on the theoretical analysis obtained in Section III, we can get the QoE coverage radius $r_{max}^{P_t}$ of a single cell given the network coverage probability.

Then, we get the coverage ratio of a single LED cell in a room of area A_{rea}. The coverage ratio at the l-th LED cell can be expressed as

$$P_l = \frac{\pi(r_{max\_l}^{P_t})^2}{A_{rea}}, \tag{32}$$

where $r_{max\_l}^{P_t}$ is the QoE coverage radius of l-th LED.

According to the coverage ratio of multiple cells expression in [18], it can be expressed as

$$P_{multi-cell} = 1 - \prod_{l=1}^{N_c}(1 - P_l), \tag{33}$$

where N_c is the number of LED cells.

In the simulation, we consider two NOMA power allocation schemes to evaluate the coverage performance.

V. SIMULATION RESULTS

In this section, we aim to shed light on the factors such as number of UEs, transmission power, UE density, PA scheme, affecting the VLC QoE network coverage probability by Monte Carlo simulation and to validate the theoretical results derived in the previous section. Simulation parameters are listed in Table 2 and adopted by related studies on VLC networks [41].

TABLE 2. Simulation parameters.

Parameter name, notation	value
Vertical separation between LED and PDs, L	$2.5[m]$
Total transmitting power, P	$0.5[W]$
Reflective index, n	1.5
Optical filter gain, T_s	1
Uniform distribution parameter, λ	0.2
LED Semi-angle at half power, $\varphi_{1/2}$	$60[deg.]$
PD FOV, ψ_{FOV}	$60[deg.]$
PD detection area, A	$1[cm^2]$
Signal bandwidth, B	$10[MHz]$
Noise PSD, N_0	$10^{-21}[A^2/Hz]$
Area of room, A_{rea}	$25[m^2]$

For single cell, we assume the existence of N UEs in the coverage area that simultaneously served by LED by using NOMA. If not otherwise specified, the PA factor of the i-th UE is $a_i^2 = 2\,(N+1-i)\,/\,(N\,(N+1))$, $i = \{1, 2, \ldots, N\}$. The UEs' locations are modeled as a uniform distribution process with the density λ. The UEs' density λ and N are related to the coverage radius r_{max}, i.e., $N = \lambda\pi r_{max}^2$.

In Fig. 3, the QoE network coverage probability versus the coverage radius are compared with different UE densities. When λ is fixed, the increase of coverage radius r_{max} leads to the increase in the number of UEs in the coverage area. From Fig. 3, we can see that when the UE density increases from 0.1 to 0.4, the coverage probability keeps decreasing in the same coverage radius. An increase in the UE density will

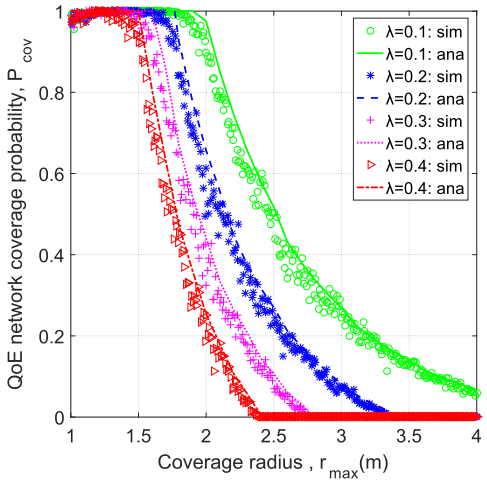

FIGURE 3. QoE network coverage probability versus UE densities and coverage radius with NOMA ($Q_t = 4$, "sim" means the results of Monte Carlo simulations, "ana" means the results of theoretical analysis simulations).

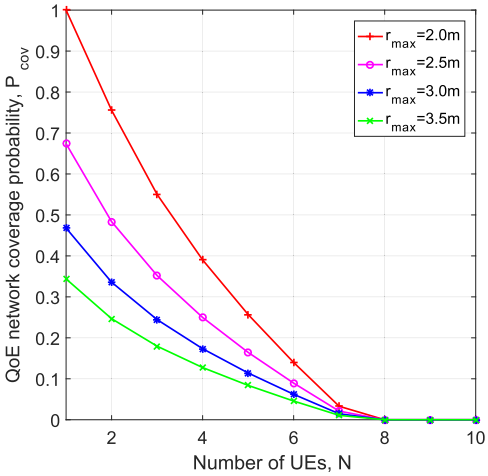

FIGURE 4. QoE network coverage probability versus number of UEs with NOMA ($Q_t = 4$).

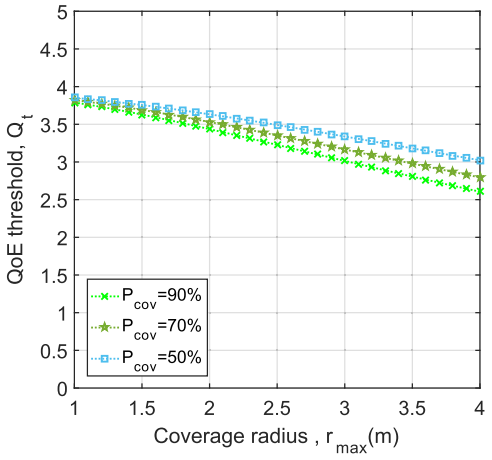

FIGURE 5. QoE threshold versus coverage radius with NOMA ($\lambda = 0.2$).

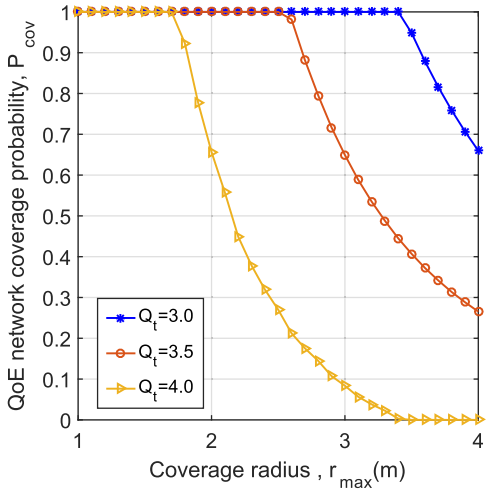

FIGURE 6. QoE network coverage probability versus coverage radius with NOMA ($\lambda = 0.2$, $Q_t = 4$).

result in the increase in the number of accessing UEs, thereby affecting coverage performance. Since the total transmitting power P is fixed, the coverage probability decreases as the coverage area expands. When more UEs access to the VLC network, each UE is allocated with less power, the coverage radius is reduced given the coverage probability.

Fig. 4 demonstrates that the coverage probability decreases as the number of UEs in a fixed coverage area. When the number of UEs is fixed and the coverage area is expanded, the UE may be far away from the LED transmitter in a larger coverage area, which makes the channel condition worse. In this case, the UE needs to be allocated more power to satisfy QoE condition, therefore, the coverage probability is reduced, too.

In Fig. 5 and Fig. 6, the effect of QoE threshold versus coverage radius on QoE coverage probability is studied. With the same coverage probability, when Q_t is reduced from 4.0 to 3.5, the coverage radius changes by 1 m, and when Q_t is reduced from 3.5 to 3.0, r_{max} also changes by 1 m. Therefore, when the network needs to accommodate more UEs, we can moderately lower the threshold. Simultaneously, we can see that the coverage probability and the coverage radius show an approximate linear relationship. This can be used to design UEs accessing algorithm in the next study, so as to reduce the delay and bad experience caused by the interrupted connections.

Fig. 7 illustrates the impact of transmission power on the coverage probability in the proposed coverage model. In Fig. 7, when the radius of the coverage area grows larger, transmission power needs to be increased to achieve the same coverage probability. With a fixed UE density, the smaller coverage area, the fewer UEs in the coverage area. Therefore, in Fig. 7, when r_{max} achieves 2 m, the transmission power is higher than 0.9 W, the coverage probability has already reached 1. The larger coverage area, the more UEs, and the higher transmission power is required. If the transmission power of LED is small at the beginning, UEs cannot access to the system. Hence, when r_{max} achieves 3.5 m and the transmission power of LED is less than 0.5 W, the coverage

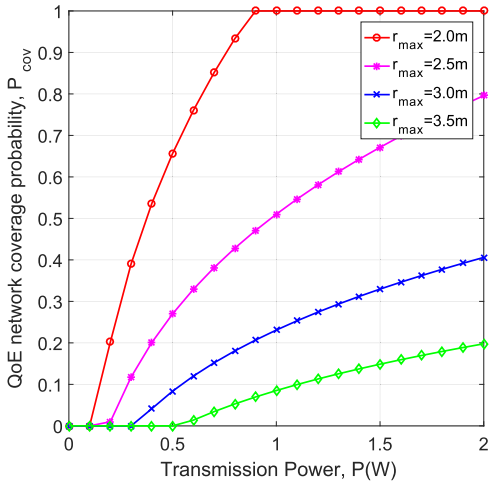

FIGURE 7. QoE network coverage probability versus transmission power with NOMA ($\lambda = 0.2$, $Q_t = 4$).

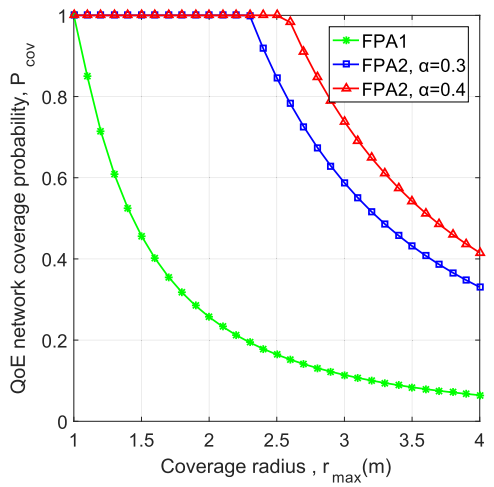

FIGURE 8. Comparison of the impact of PA factors on coverage performance with NOMA.

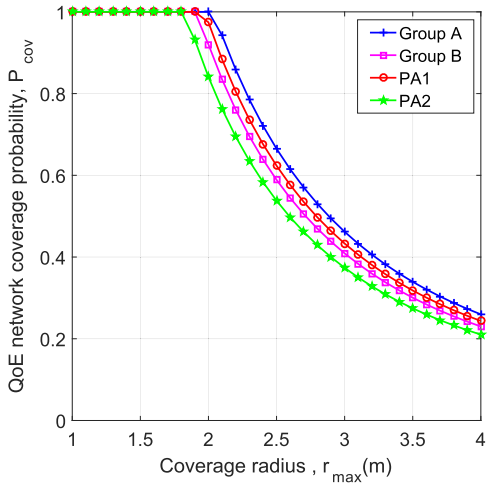

FIGURE 9. Comparison of the impact of PA and UE groups on coverage performance with user pairing.

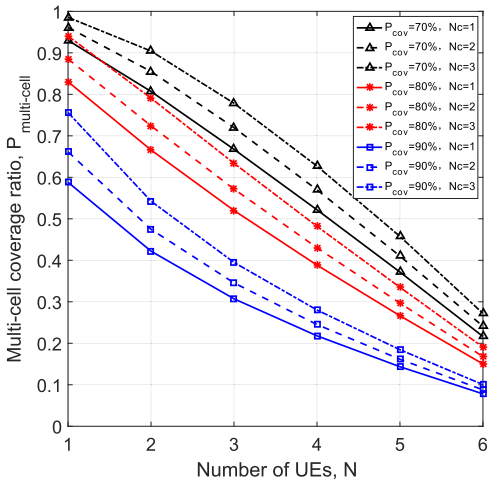

FIGURE 10. Multi-cell coverage ratio changes as the number of UEs with FPA1.

probability is always 0. In order to maximize the efficiency of the LED layout, it can be seen from Fig. 7 that the appropriate power is selected within a certain coverage area to optimize the coverage performance.

Fig. 8 shows the coverage probability for two PA schemes. The first fixed power allocation (FPA1) factor $a_i = \sqrt{2(N-i+1)/(N(N+1))}$, where N is the number of UEs in the coverage area. The second fixed power allocation (FPA2) factor $a_i = \alpha a_{i-1}$[42], where α is a constant, we consider two values, 0.3 and 0.4, respectively. Both strategies ensure that the constraint $\sum_{i=1}^{N} a_i^2 = 1$. From Fig. 8, it can be seen that the FPA2 performs better than FPA1 as it compensates for channel difference among UEs. In the case of the same coverage area, the coverage probability of adopting FPA2 is higher than that of FPA1.

Fig. 9 compares the performance of user pairing with different groups of UEs and different PA methods. First of all, we select two groups of UEs in the coverage area. Group A is defined as the group of two UEs in the coverage area, that the distance between them is the farthest among any two UEs, i.e., $U(c,d) = \arg\max_{c,d} l_{cd}$, where l_{cd} is the distance between c-th and d-th UE. Group B is the nearest distance group, $U(c,d) = \arg\min_{c,d} l_{cd}$. The same PA methods are utilized in Group A and Group B. Then, we compare two PAs for Group A, PA1: $a_c^2 = 9/10, a_d^2 = 1/10$ and PA2: $a_c^2 = 3/4, a_d^2 = 1/4$, respectively. As we can see from Fig. 9, Group A performs better than Group B with higher coverage probability, and PA1 performs better than PA2, these can be explained as follows. When two UEs are far apart or the power allocation factor decreases, more power will be given to the UE with a better channel condition, which leads to improvement in a system throughput. Therefore, the coverage probability can be improved by grouping UEs with larger channel differences.

Figs. 10-12 compare the coverage ratio of FPA1 with that of FPA2 for multi-cell network comprising randomly deployed UEs with P_{cov}=70%, 80%, 90%, N_c=1, 2, 3. We can see that the variation curve of coverage probability is close

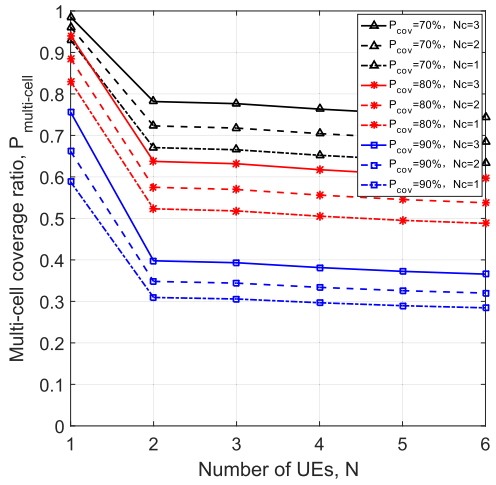

FIGURE 11. Multi-cell coverage ratio changes as the number of UEs with FPA2.

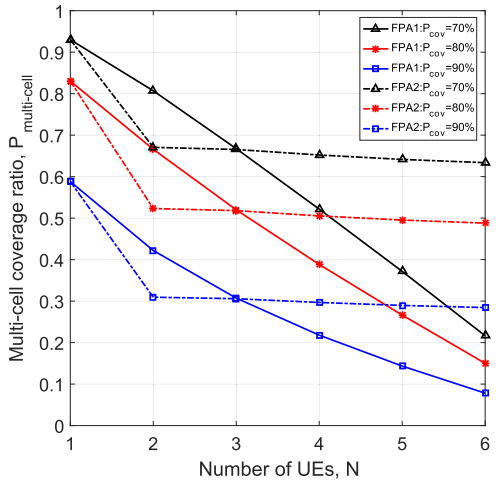

FIGURE 12. Compare multi-cell coverage ratio with FPA1 and FPA2.

to linear change when using FPA1, so it can be used to provide theoretical basis for the optimization research of multiple UEs access. Because the QoE probability coverage area is defined as all the UEs in the area can satisfy the QoE condition with a given network coverage probability, the QoE coverage radius is extended when reducing the network coverage probability, i.e., coverage probability threshold. In Fig. 10-12, when the coverage probability is 70%, the coverage ratio is higher than that 80% and 90%. In related study, the corresponding power allocation can be selected according to requirements, so as to achieve the goal of optimizing the overall performance.

VI. CONCLUSION

In this paper, we discuss the indoor VLC network coverage performance. Using QoE as the evaluation metric, we propose the QoE probability coverage model. We study how the factors including number of UEs, UE density, transmission power, etc., affect the QoE network coverage probability. At first, we analyze the coverage probability theoretically derived in one LED cell by utilizing NOMA and user pairing. Then, we further analyze the situation when multiple cells are applying in a room, simultaneously. Through the simulation results obtained, we can give effective prediction scheme for the study of multiple access and network handover to enhance the efficiency of UE access network and improve handover delay.

REFERENCES

[1] T. Komine and M. Nakagawa, "Fundamental analysis for visible-light communication system using LED lights," *IEEE Trans. Consum. Electron.*, vol. 50, no. 1, pp. 100–107, Feb. 2004.
[2] J. Grubor, S. Randel, K.-D. Langer, and J. W. Walewski, "Broadband information broadcasting using LED-based interior lighting," *J. Lightw. Technol.*, vol. 26, no. 24, pp. 3883–3892, Dec. 15, 2008.
[3] H. Haas, L. Yin, Y. Wang, and C. Chen, "What is LiFi?" *J. Lightw. Technol.*, vol. 34, no. 6, pp. 1533–1544, Mar. 15, 2016.
[4] A. Jovicic, J. Li, and T. Richardson, "Visible light communication: Opportunities, challenges and the path to market," *IEEE Commun. Mag.*, vol. 51, no. 12, pp. 26–32, Dec. 2013.
[5] X. Bao, G. Yu, J. Dai, and X. Zhu, "Li-Fi: Light fidelity-a survey," *Wireless Netw.*, vol. 21, no. 6, pp. 1879–1889, Jan. 2015.
[6] J. Miyakoshi, "Cellular and molecular responses to radio-frequency electromagnetic fields," *Proc. IEEE*, vol. 101, no. 6, pp. 1494–1502, Jun. 2013.
[7] B. Wang, "Coverage problems in sensor networks: A survey," *ACM Comput. Surv.*, vol. 43, no. 4, pp. 32:1–32:53, Oct. 2011.
[8] Q. Yang, S. He, J. Li, J. Chen, and Y. Sun, "Energy-efficient probabilistic full coverage in wireless sensor networks," in *Proc. IEEE Global Commun. Conf. (GLOBECOM)*, Dec. 2012, pp. 591–596.
[9] H. Prabhat Gupta, S. V. Rao, and T. Venkatesh, "Critical sensor density for partial coverage under border effects in wireless sensor networks," *IEEE Trans. Wireless Commun.*, vol. 13, no. 5, pp. 2374–2382, May 2014.
[10] J. Yu, S. Wan, X. Cheng, and D. Yu, "Coverage contribution area based k-coverage for wireless sensor networks," *IEEE Trans. Veh. Technol.*, vol. 66, no. 9, pp. 8510–8523, Sep. 2017.
[11] H. Xu, J. Zhu, and B. Wang, "On the deployment of a connected sensor network for confident information coverage," *Sensors*, vol. 15, no. 5, pp. 11277–11294, May 2015.
[12] B. Wang, J. Zhu, L. T. Yang, and Y. Mo, "Sensor density for confident information coverage in randomly deployed sensor networks," *IEEE Trans. Wireless Commun.*, vol. 15, no. 5, pp. 3238–3250, May 2016.
[13] L.-Y. Liu, Z.-G. Ma, Y. Xue, W.-B. Yan, and Y.-Y. Li, "Research on coverage probability in ultra-dense 5G heterogeneous cellular networks based on Poisson clustered process," *Wireless Pers. Commun.*, vol. 95, no. 3, pp. 2915–2930, Jan. 2017.
[14] H. Zhang, Y. Chen, Z. Yang, and X. Zhang, "Flexible coverage for backhaul-limited ultradense heterogeneous networks: Throughput analysis and η-optimal biasing," *IEEE Trans. Veh. Technol.*, vol. 67, no. 5, pp. 4161–4172, May 2018.
[15] V. M. Nguyen and M. Kountouris, "Coverage and capacity scaling laws in downlink ultra-dense cellular networks," in *Proc. IEEE Int. Conf. Commun. (ICC)*, May 2016, pp. 1–7.
[16] *Ultra Dense Network (UDN) White Paper*, Nokia, Espoo, Finland, 2017.
[17] M. Obeed, A. M. Salhab, M.-S. Alouini, and S. A. Zummo, "On optimizing VLC networks for downlink multi-user transmission: A survey," *IEEE Commun. Surveys Tuts.*, vol. 21, no. 3, pp. 2947–2976, 3rd Quart., 2019.
[18] A. Vavoulas, H. G. Sandalidis, T. A. Tsiftsis, and N. Vaiopoulos, "Coverage aspects of indoor VLC networks," *J. Lightw. Technol.*, vol. 33, no. 23, pp. 4915–4921, Dec. 1, 2015.
[19] M. T. Niaz, F. Imdad, S. Kim, and H. S. Kim, "Deployment methods of visible light communication lights for energy efficient buildings," *Opt. Eng.*, vol. 55, no. 10, Oct. 2016, Art. no. 106113.
[20] C. Chen, W.-D. Zhong, and D. Wu, "On the coverage of multiple-input multiple-output visible light communications [invited]," *J. Opt. Commun. Netw.*, vol. 9, no. 9, pp. D31–D41, Aug. 2017.
[21] H. Tabassum and E. Hossain, "Coverage and rate analysis for co-existing RF/VLC downlink cellular networks," *IEEE Trans. Wireless Commun.*, vol. 17, no. 4, pp. 2588–2601, Apr. 2018.
[22] H. Haas, "High-speed wireless networking using visible light," *SPIE Newsroom*, vol. 1, pp. 1–3, Apr. 2013.

[23] L. Yin and H. Haas, "Coverage analysis of multiuser visible light communication networks," *IEEE Trans. Wireless Commun.*, vol. 17, no. 3, pp. 1630–1643, Mar. 2018.
[24] S. Shashikant, P. Garg, and P. K. Sharma, "Interference mitigation technique with coverage improvement in indoor VLC system," *Trans. Emerg. Telecommun. Technol.*, vol. 30, no. 2, Sep. 2018, Art. no. e3511.
[25] Z. Ding, Z. Yang, P. Fan, and H. V. Poor, "On the performance of non-orthogonal multiple access in 5G systems with randomly deployed users," *IEEE Signal Process. Lett.*, vol. 21, no. 12, pp. 1501–1505, Dec. 2014.
[26] Y. Liu, Z. Qin, M. Elkashlan, Z. Ding, A. Nallanathan, and L. Hanzo, "Non-orthogonal multiple access for 5G and beyond," *Proc. IEEE*, vol. 105, no. 12, pp. 2347–2381, Dec. 2017.
[27] R. C. Kizilirmak, C. R. Rowell, and M. Uysal, "Non-orthogonal multiple access (NOMA) for indoor visible light communications," in *Proc. 4th Int. Workshop Opt. Wireless Commun. (IWOW)*, Sep. 2015, pp. 98–101.
[28] B. Lin, X. Tang, Z. Ghassemlooy, C. Lin, M. Zhang, Z. Zhou, Y. Wu, and H. Li, "A NOMA scheme for visible light communications using a single carrier transmission," in *Proc. 1st South Amer. Colloq. Visible Light Commun. (SACVLC)*, Nov. 2017, pp. 1–4.
[29] D. O'Brien, R. Turnbull, H. Le Minh, G. Faulkner, O. Bouchet, P. Porcon, M. El Tabach, E. Gueutier, M. Wolf, L. Grobe, and J. Li, "High-speed optical wireless demonstrators: Conclusions and future directions," *J. Lightw. Technol.*, vol. 30, no. 13, pp. 2181–2187, Jul. 1, 2012.
[30] T. Fath and H. Haas, "Performance comparison of MIMO techniques for optical wireless communications in indoor environments," *IEEE Trans. Commun.*, vol. 61, no. 2, pp. 733–742, Feb. 2013.
[31] J. Kahn and J. Barry, "Wireless infrared communications," *Proc. IEEE.*, vol. 85, no. 2, pp. 265–298, Feb. 1997.
[32] L. Yin, W. O. Popoola, X. Wu, and H. Haas, "Performance evaluation of non-orthogonal multiple access in visible light communication," *IEEE Trans. Commun.*, vol. 64, no. 12, pp. 5162–5175, Dec. 2016.
[33] H. Dadheech, B. Jennings, and J. Dunne, "A call quality assessment and analysis framework for video telephony applications in enterprise networks," in *Proc. Global Inf. Infrastructure Symp. (GIIS)*, Oct. 2013, pp. 1–6.
[34] J. A. Bergstra and C. A. Middelburg, *The E-model: A Computational Model for Use in Transmission Planning*, document ITU-T Recommendation G.107, 2003, pp. 183–211.
[35] S. Sengupta, M. Chatterjee, and S. Ganguly, "Improving quality of VoIP streams over WiMax," *IEEE Trans. Comput.*, vol. 57, no. 2, pp. 145–156, Feb. 2008.
[36] A. B. Reis, J. Chakareski, A. Kassler, and S. Sargento, "Distortion optimized multi-service scheduling for next-generation wireless mesh networks," in *Proc. INFOCOM IEEE Conf. Comput. Commun. Workshops*, Mar. 2010, pp. 1–6.
[37] *Final Report From the Video Quality Experts Group on the Validation of Objective Models of Video Quality Assessment, Phase II (FR-TV2)*, document ITU-T SG09, TVQE Group, 2003.
[38] C. A. Courcoubetis, A. Dimakis, and M. I. Reiman, "Providing bandwidth guarantees over a best-effort network: Call-admission and pricing," in *Proc. IEEE Conf. Comput. Commun. 20th Annu. Joint Conf. IEEE Comput. Commun. Soc. (INFOCOM)*, vol. 1, Apr. 2001, pp. 459–467.
[39] H. Marshoud, S. Muhaidat, P. C. Sofotasios, S. Hussain, M. A. Imran, and B. S. Sharif, "Optical non-orthogonal multiple access for visible light communication," *IEEE Wireless Commun.*, vol. 25, no. 2, pp. 82–88, Apr. 2018.
[40] Z. Ding, P. Fan, and H. V. Poor, "Impact of user pairing on 5G nonorthogonal multiple-access downlink transmissions," *IEEE Trans. Veh. Technol.*, vol. 65, no. 8, pp. 6010–6023, Aug. 2016.
[41] Z. Ghassemlooy, W. Popoola, and S. Rajbhandari, *Optical Wireless Communications: System and Channel Modelling With MATLAB*. Boca Raton, FL, USA: CRC Press, 2012.
[42] Z. Ding, M. Peng, and H. V. Poor, "Cooperative non-orthogonal multiple access in 5G systems," *IEEE Commun. Lett.*, vol. 19, no. 8, pp. 1462–1465, Aug. 2015.

JUAN LI is currently pursuing the M.Sc. degree with the School of Computer Science and Communication Engineering, Jiangsu University, Zhenjiang, China. Her current research focuses on the visible light communications.

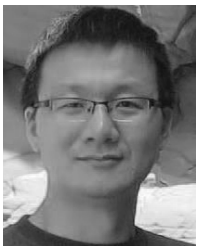

XU BAO received the B.E. and M.E. degrees in communication engineering from Jiangsu University, Zhenjiang, China, in 2003 and 2006, respectively, and the Ph.D. degree from the National Mobile Communications Research Laboratory, Southeast University, Nanjing, China, in 2011. From 2013 to 2014, he held a postdoctoral position at the Georgia Institute of Technology, Atlanta, GA, USA. He is currently a Professor with the School of Computer Science and Communication Engineering, Jiangsu University. His research interests include visible light communications, wireless network design, and heterogeneous networks.

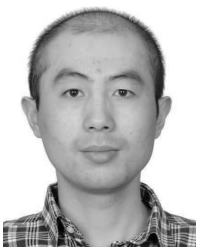

WANCE ZHANG received the Ph.D. degree from the National Mobile Communications Research Laboratory, Southeast University, Nanjing, China, in 2015. From 2013 to 2014, he was a Visiting Student with the Department of Electronics, University of York, York, U.K. From 2015 to 2016, he was a Postdoctoral Researcher with CETUC, PUC-Rio, Brazil. Since 2016, he has been an Associate Professor with Jiangsu University, Zhenjiang, China. His research interests include distribute antenna systems and massive MIMO. He served as a TPC Member for the IEEE ICC 2015–2017 and the Session Chair for the IEEE SAM 2016.

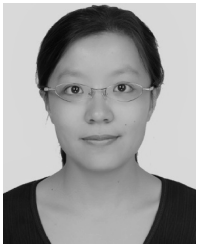

NAN BAO received the B.S. degree from the University of Electronic Science and Technology of China (UESTC), Chengdu, in 2008, and the Ph.D. degree from Southeast University (SEU), Nanjing, in 2014. She is currently a Lecturer with the School of Internet of Things, Nanjing University of Posts and Telecommunications (NJUPT). Her research interests include wireless resource management and wireless communication network technology.